

Applying Lambert problem to association of radar-measured orbit tracks of space objects

Lei Liu¹, Bin Li¹, Jun-Yu Chen¹, Xiang-Xu Lei³, Guang-Yu Zhao¹ and Ji-Zhang Sang^{1,2}

¹ School of Geodesy and Geomatics, Wuhan University, Wuhan 430079, China; bli@sgg.whu.edu.cn

² Collaborative Innovation Center for Geospatial Technology, Wuhan 430079, China

³ School of Civil and Architectural Engineering, Shandong University of Technology, Zibo 255000, China

Received 2021 April 30; accepted 2021 September 17

Abstract Thousands of orbit tracks of space objects are collected by a radar each day, and many may be from uncatalogued objects. As such, it is an urgent demand to catalogue the uncatalogued objects, which requires to determine whether two or more un-correlated tracks (UCTs) are from the same object. This paper proposes to apply the Lambert problem to associate two radar-measured orbit tracks of LEO and HEO objects. A novel method of position correction is proposed to correct the secular and short periodic effects caused by the J_2 perturbation, making the Lambert problem applicable to perturbed orbit tracks. After that, an orbit selection method based on the characteristics of residuals solves the multiple-revolution Lambert problem. Extensive experiments with simulated radar measurements of LEO and HEO objects are carried out to assess the performance of the proposed method. It is shown that the semi-major axis can be determined with an error less than 200 m from two tracks separated by 4 days. The true positive (TP) rates for associating two LEO tracks apart by less than 6 days are 94.2%. The TP rate is still at 73.1% even for two tracks apart by 8–9 days. The results demonstrate the strong applicability of the proposed method to associate radar measurements of uncatalogued objects.

Key words: celestial mechanics — methods: analytical — techniques: miscellaneous — surveys

1 INTRODUCTION

The mega low-Earth orbiting (LEO) satellite constellations in deployment and planning will make the near-Earth space crowded more than ever. Many newly launched satellites appear to show the characteristics of small in size and large in number. In addition, every space launch is accompanied by the generation of space debris. As a result, operational satellites are more likely involving space collisions, and the space sustainability is increasingly threatened (Xu & Xiong 2014). It is a demand to not only maintain a catalogue of space objects but also catalogue new objects from their surveillance data as quickly as possible for the sake of space safety management (Huang et al. 2012).

At present, space object surveillance is mainly operated with the optical and radar techniques, with the latter being dominant for LEO objects because of its capability of simultaneously tracking multiple objects and being all-weather operational (Jiang et al. 2017). When an object passes the field of view (FOV) of either a radar or optical sensor, its orbit track could be detected if the detection conditions are met (Liu et al. 2020). The track or tracklet usually consists of a number of data points. For the

radar, each data point may be expressed as:

$$\xi = \{t, \rho, \beta, el\}, \quad (1)$$

where t is the detection time, ρ the one-way range, β the azimuth, and el the elevation. The radar station position is $\mathbf{P}_{\text{site}} = \{\phi, \lambda, h\}$, where ϕ is the geodetic latitude, λ the geodetic longitude, and h the geodetic height in an Earth-centered Earth-fixed (ECEF) coordinate system. Usually, the range is more accurate than the azimuth and elevation (Gronchi et al. 2015b). Depending on the FOV size, the location of the track within the FOV, and the relative motion speed of the object with respect to the sensor, the track may only have a duration of tens of seconds in time.

Given a track, it will be processed in a few steps. The first step is to associate the track to a catalogued object. If success, the track can then be used to update the orbit of the associated object (Agapov 2001). Otherwise, the track becomes an un-correlated track (UCT), which is most likely from an uncatalogued object. A preliminary estimation of the orbital elements would be made first for the UCT, which is called initial orbit determination (IOD) (Maruskin et al. 2009; Lee et al. 2020). The IOD

elements from the use of a single track usually have large errors that would make the elements practically of little use. Therefore, the track would have to be associated with other UCTs from the same object (Memon et al. 2020), such that multiple tracks are processed to determine the orbital elements of the object in an accuracy meeting the cataloguing requirement.

The IOD problem for a radar track is easier than that for an angles-only track, since the radar track provides three dimensional (3D) positions of the object. One could employ the classical methods to solve the standard Lambert problem given two positions, such as Gibbs method or Herrick-Gibbs method given three positions. These methods and the discussions can be found in e.g., Escobal (1969) and Vallado & McClain (1997). There are various methods to solve the Lambert problem. Among them, Battin and Gooding methods have been widely used (Battin 1977; Gooding 1990). Recently, Izzo proposed a low computational complexity algorithm with Householder iterative method (Izzo 2015). Gronchi et al. used algebraic integrals of the two-body problem to calculate the initial orbital elements (Gronchi et al. 2015a). Ma et al. selected a perturbed Keplerian dynamics model to correct the angular measurements and to determine the initial orbital elements of LEO satellite (Ma et al. 2018). Feng proposed a novel quasi linearization-local variational iteration method to solve the perturbed Lambert problem (Feng et al. 2021).

The track association is normally operated to two UCTs (Vananti et al. 2017). One may make association between measurements of two tracks, between measurements of a track and IOD elements of another track, or between IOD element sets of two tracks which appear a practically more applicable approach. The Covariance-based Track Association (CBTA) uses a Mahalanobis distance between two IOD tracks at a common epoch as a metric to determine the association of the two tracks (Hill et al. 2014). In the distance computation, the covariance matrices of the position and velocity vectors are needed, which may be a problem to the use of the method, since the covariance is usually unreliable or even unknown. The geometrical approach to associate two IOD elements proposed by Lei et al. avoids the use of the covariance, and its applicability is validated in the identification of uncatalogued LEO objects detected by a ground electro-optical array (Lei et al. 2018; Lei 2021).

For the association of two very-short radar tracks, Reihls et al. (2020) proposed an IOD method from two tracks in which the influences of J_2 secular perturbation on the right ascension of ascending node, perigee argument and mean anomaly are considered, and used Mahalanobis distance containing range rates to solve the multiple-revolution orbit determination problem. The accuracy of the determined semi-major axis from the two-track orbit

determination is about 600 m for 800 km LEO object, and worse than 10 km for HEO object (fig. 26 in Reihls et al. 2020). The TP rate is 84.8% for associating two tracks of 800 km LEO object, and 76.0% for HEO object (table 3 in Reihls et al. 2020).

This paper proposes to use exclusively the Lambert problem to perform the association of two radar tracks which also determines a set of accurate orbital elements if the two tracks are from the same object. The classical Lambert problem is restricted to the two-body orbit. To make the Lambert problem applicable to two positions separated by a few days, the orbit perturbations must be considered. It is known that the J_2 perturbation is the dominant one for LEO orbits. Over the time span of a few days, the J_2 perturbation can be decomposed into the secular and short-periodic variations in the orbital elements, which are computable if the orbital elements are known. For the UCT track association, only the IOD elements from a single track are available. In the paper, a procedure to correct the perturbed positions for the J_2 perturbation effects based on the IOD elements of a radar track is developed. For the near-circular orbit, it is sufficient to consider the secular effects on the right-ascension of ascending node, perigee argument and the mean anomaly. This paper considers the orbit eccentricity that the effects on the true anomaly and geocentric distance are derived. In addition, the short-periodic effects are accounted for in the iteration process. After the perturbation correction, the positions can be regarded from a two-body orbit, and thus the Lambert problem can be solved. It is noted that the IOD elements for computing the J_2 perturbation are determined by applying the Lambert problem to two positions within a single track.

In our work, the method by Gooding (1990) is mainly used to solve the Lambert problem. Gooding's procedure uses Halley's cubic iteration process to evaluate the unknown parameter, and initial value of the unknown parameter is selected to make sure the iteration quickly converges to an accurate result. With this, the procedure solves the Lambert problem with high efficiency and precision.

In what follows, the Lambert problem-based track association method is presented in Section 2. The simulation experiments of two-track orbit determination and track association for LEO and HEO objects are carried out, and the results are analyzed in Section 3. Conclusions are given in Section 4.

2 METHOD

Given two radar tracks, $\{\xi_i^1, i = 1, 2, \dots, i_1\}$ and $\{\xi_i^2, i = 1, 2, \dots, i_2\}$, whether they come from the same object should be determined in the track association. The radar station positions observing the two tracks are P_{site}^1 and P_{site}^2 , respectively. The two tracks may be from the same

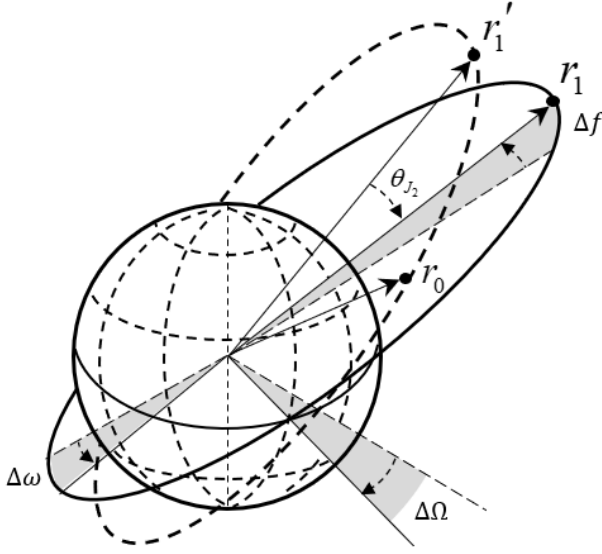


Fig. 1 Orbital change due to J_2 secular perturbation.

object or from two different objects. The two sites may be the same. To apply the Lambert problem to the radar track data, the observations should be converted to the 3D positions in an inertial coordinate system, which is defined at the first epoch of the first track in this paper. The conversion can be performed as follows.

The radar data point is first converted to the local north-east-up coordinate system, \mathbf{P}_{NEU} , at the radar station $\mathbf{P}_{siteECEF}$,

$$\mathbf{P}_{NEU} = \begin{bmatrix} \rho \cos el \cos \beta \\ \rho \cos el \sin \beta \\ \rho \sin el \end{bmatrix}. \quad (2)$$

\mathbf{P}_{NEU} is then transformed to the position with respect to the radar station in the ECEF coordinate system, where the coordinate transformation matrix is expressed as

$$\mathbf{R}_{NEU \rightarrow ECEF} = \begin{bmatrix} \sin \phi \cos \lambda & -\sin \lambda & \cos \phi \cos \lambda \\ \sin \phi \sin \lambda & \cos \lambda & \cos \phi \sin \lambda \\ -\cos \phi & 0 & \sin \phi \end{bmatrix}. \quad (3a)$$

This gives the position of the track point in the ECEF coordinate system as

$$\mathbf{P}_{ECEF} = \mathbf{P}_{siteECEF} + \mathbf{R}_{NEU \rightarrow ECEF} \cdot \mathbf{P}_{NEU}. \quad (3b)$$

Finally, the position of the track point in the inertial coordinate system at the tracking time t is obtained as

$$\mathbf{P}_{TOD} = [\mathbf{P}(t)] [\mathbf{N}(t)] [\mathbf{R}(t)] [\mathbf{W}(t)] \mathbf{P}_{ECEF}, \quad (4)$$

where \mathbf{P} and \mathbf{N} are the precession and nutation matrices at epoch t , respectively, \mathbf{R} the matrix considering the Earth rotation, and \mathbf{W} the polar-motion matrix. When two positions in the inertial coordinate system are given, a set of orbital elements may be calculated if the two positions are from the same object. The two-point boundary value

Table 1 Two Position Vectors on a Two-body Orbit

Position ID	Epoch	X(m)	Y(m)	Z(m)
1	0:00:00	-2320090.4	6339450.1	3897490.8
2	10:39:52	6168644.5	-3579260.8	-3159956.7

Table 2 Orbit Parameters and Number of Orbit Revolutions (Revs)

a (km)	e	i ($^\circ$)	Ω ($^\circ$)	Orbital Period (h)	Revs
9403.7	0.305025	150	200	2.521	4.230
8736.3	0.218140	30	20	2.257	4.724
8037.6	0.079087	150	200	1.992	5.354
7800.0	0.001000	30	20	1.904	5.600

problem in the two-body orbit dynamics is the classical Lambert problem (Andrew 1975; Ha 2001).

Applying the Lambert problem to determine the association of two radar tracks needs to consider a few apparent issues: (a) a number of orbit revolutions may have passed between the two tracks; (b) the orbit perturbation prevents the direct use of the positions from the two tracks; (c) how to determine the association. These issues are discussed in the following sub-sections.

2.1 Position Correction for J_2 Perturbation

2.1.1 Influence of J_2 perturbation

The problem of determining the IOD elements from two positions of a single track of only a few minutes in duration can be simply treated as a two-body problem. For the two-track association problem, the separation time between two tracks could be a few days. In this case, it certainly cannot be treated as a two-body problem because of the orbit perturbation. For LEO orbits, the main disturbing force is the J_2 perturbation representing the oblateness of the Earth. It is conventional to decompose the J_2 perturbation into the secular and periodic terms. The secular effects of J_2 perturbation on the six Keplerian orbital parameters are as follows (Vallado & McClain 1997)

$$\begin{cases} \dot{a} = 0 \\ \dot{e} = 0 \\ \dot{i} = 0 \\ \dot{\Omega} = -\frac{3}{2} \frac{J_2 a_E^2}{p^2} n \cos i \\ \dot{\omega} = \frac{3}{2} \frac{J_2 a_E^2}{p^2} n \left(2 - \frac{5}{2} \sin^2 i\right) \\ \dot{M} = \frac{3}{2} \frac{J_2 a_E^2}{p^2} n \left(1 - \frac{3}{2} \sin^2 i\right) \sqrt{1 - e^2} \end{cases}, \quad (5)$$

where $(a, e, i, \Omega, \omega, M)$ are the semi major axis (SMA), the eccentricity, the inclination and the right ascension of the ascending node (RAAN), the argument of perigee, and the mean anomaly, respectively, $(\dot{a}, \dot{e}, \dot{i}, \dot{\Omega}, \dot{\omega}, \dot{M})$ represent the change rates of the Keplerian orbital elements caused by the J_2 secular perturbation, a_E is the Earth radius,

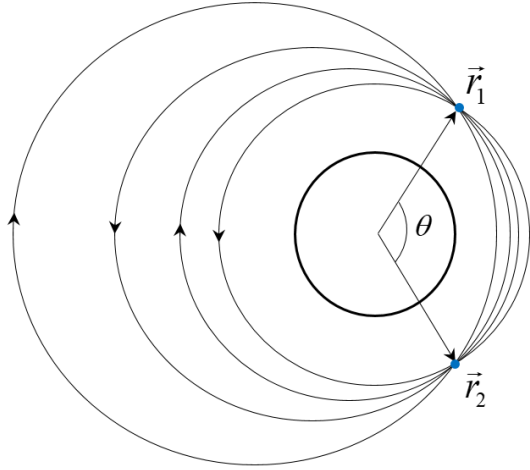


Fig. 2 Solutions to the multiple-revolution Lambert problem.

Table 3 Mean Orbital Elements

$a(\text{km})$	e	$i(^{\circ})$	$\Omega(^{\circ})$	$\omega(^{\circ})$	$M(^{\circ})$
7000.0	0.001	30.0	20.0	40.0	50.0

$p = a(1 - e^2)$ is the semi-latus rectum, and n is the mean motion.

According to the above formula, the secular influence of the J_2 perturbation on the object orbit is on Ω , ω , and M . The orbit plane rotates at the constant rate $\dot{\Omega}$, the perigee rotates at $\dot{\omega}$, and the mean anomaly also changes at \dot{M} in addition to the mean motion. Clearly, the change rates are related to the SMA, eccentricity and inclination of the object. Figure 1 illustrates the orbits of an object and the object positions at t_0 and $t_1 = t_0 + \Delta t$, considering the J_2 secular perturbation, where $\Delta t = 2d$. The example clearly shows the effects of the J_2 secular perturbation on the positions. Assuming a set of mean Keplerian elements of a LEO object at t_0 is $\{a = 6800.0 \text{ km}, e = 0.001, i = 30^{\circ}, \Omega = 20^{\circ}, \omega = 40^{\circ}, M = 50^{\circ}\}$, and considering only the J_2 secular perturbation, the positions at t_0 and $t_1 = t_0 + 2d$ and the orbital elements at t_1 , can be computed. It is seen that the orbit plane has rotated around the Z axis by $\Delta\Omega = -0.241^{\circ}$, the perigee has changed by $\Delta\omega = 0.382^{\circ}$, and the mean anomaly at t_1 has an additional change of $\Delta M = 0.174^{\circ}$.

Therefore, the two positions, r_0 and r_1 , cannot be processed in the standard Lambert problem. One of them should be corrected for the J_2 secular perturbation, as well as the short-periodic perturbation if possible, in the way discussed in the next.

2.1.2 Position correction

Figure 1 has shown the differences between two orbits 2 days apart due to the J_2 secular perturbation. In fact, we can also consider the J_2 short-periodic effects in the orbital

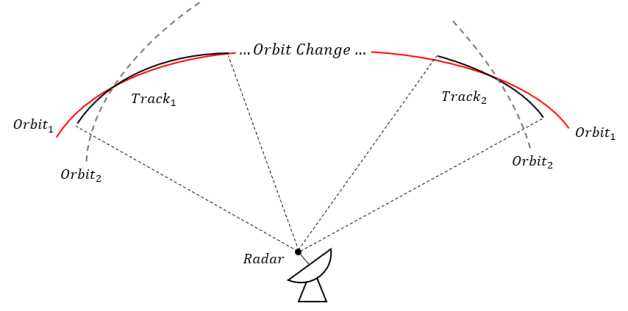


Fig. 3 Schematic diagram of orbit selection.

elements, that will result in slightly different osculating orbits.

If the mean orbital elements at an epoch are exactly known, the J_2 perturbation effects on the position at any epoch can be easily accounted for using the well-established perturbation theory (Liu 2006; Vallado & McClain 1997). That is, the mean elements at the epoch of interest are computed first by considering the secular effects, and then the osculating elements are recovered by considering the periodic effects.

For the problem of associating two radar UCTs, exact mean elements are not known since the IOD elements estimated from the observed positions of a single short track contain large errors. Experiments show that the magnitudes of the IOD element errors differ significantly from one track to another. One may propagate the IOD elements of the first track to the time of the second track in which the J_2 perturbation is considered, and then compute a Mahalanobis distance using positions computed from the propagated elements, observed positions and their covariances to make association decision. The large uncertainties in the IOD elements would be a cause of concern on the confidence whether two UCTs are correctly associated.

Therefore, we propose to determine the accurate orbital elements from 2 observed positions in two UCTs by the Lambert problem. The prerequisite to this process is to account for the perturbation effects on the observed positions. Considering the possible large errors in the estimated IOD elements, we propose an iterative procedure to correct the observed positions for the dominant J_2 perturbation.

Assume that the IOD elements of the first track have been determined, and the secular change rates $\dot{\Omega}$, $\dot{\omega}$, \dot{M} can then be computed. It is seen from Figure 1, the two osculating orbit planes are separated by $\Delta\Omega = \dot{\Omega} \cdot \Delta t$, where $\Delta t = t_1 - t_0$. This difference can be easily corrected by a rotation of $\Delta\Omega$ around the ΔZ axis in the inertial coordinate system, such that the position at t_1 now is transferred into the orbit plane at t_0 . However, the perigee of the rotated orbit has a difference of $\Delta\omega = \dot{\omega} \cdot \Delta t$ from the perigee of the orbit at t_0 . A rotation of $\Delta\omega$ around

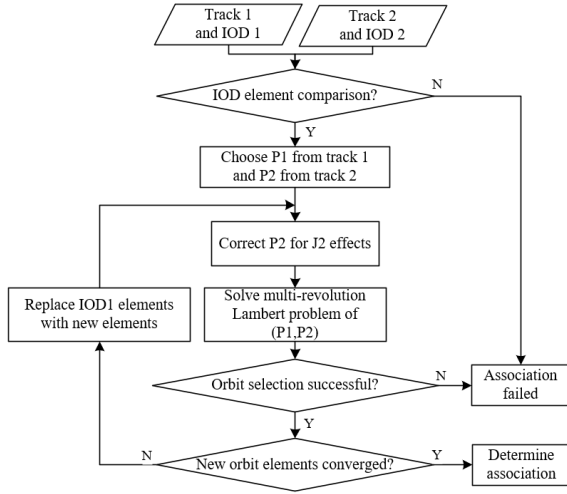


Fig. 4 Program flowchart of two-track association.

the normal to the orbit plane will make the two perigees aligned. Finally, a rotation of $\Delta M = \dot{M} \cdot \Delta t$ around the normal would correct the change in the position due to the J_2 secular perturbation effects on the mean anomaly.

It has to be noted that it is the true anomaly, rather than the mean anomaly, has a change Δf on the orbit, as shown in Figure 1. Given the perturbed mean anomaly M_1 at t_1 and $M'_1 = M_1 - \Delta M$, Δf can be computed as below

$$\begin{cases} E_1 - e \sin E_1 = M_1, E'_1 - e \sin E'_1 = M'_1 \\ \sin f_1 = \frac{\sin E_1 \sqrt{1-e^2}}{1-e \cos E_1}, \sin f'_1 = \frac{\sin E'_1 \sqrt{1-e^2}}{1-e \cos E'_1} \\ \Delta f = f_1 - f'_1 \end{cases}, \quad (6)$$

where e is the orbit eccentricity either estimated by the IOD method at the beginning or estimated from two positions in two tracks at a later iteration step. Another key point is that the change of true anomaly not only changes the relative position of the object with respect to the perigee, but also changes the geocentric distance by Δr . Δr may be ignored if the orbit is near circular, but it has to be accounted for if the orbit is eccentric. One equation to compute Δr from Δf is

$$\Delta r = \frac{er \cdot \sin f}{1 + e \cos f} \cdot \Delta f. \quad (7)$$

Combining all the above corrections together, we have the equation to correct the perturbed position at t_1 for the J_2 secular perturbation effects

$$\mathbf{r}'_1 = \mathbf{M}_\theta \mathbf{r}_1, \quad (8a)$$

$$\begin{aligned} \mathbf{M}_\theta = & \left(1 - \frac{\Delta r}{r}\right) R_Z(-\Omega) R_X(-i) R_Z(\Delta\omega + \Delta f) \\ & \times R_X(i) R_Z(\Omega) R_Z(\Delta\Omega), \end{aligned} \quad (8b)$$

where \mathbf{r}_1 is the perturbed position at t_1 , $R_X(i)R_Z(\Omega)$ transforms the inertial coordinate system into the orbital

Table 4 Orbit Determination Accuracy with Two Noisy Positions

$H_{perigee}$ (km)	Eccentricity	Δt (h)	$RMS_{\hat{a}}$ (m)	$RMS_{\hat{i}}$ (")	$RMS_{\hat{\Omega}}$ (")
500	0.001	96.21	1.02	5.87	40.34
	0.1	95.95	1.53	9.68	99.54
	0.7	96.05	10.19	203.43	633.82
700	0.001	97.20	1.35	8.09	96.55
	0.1	96.33	1.70	10.76	132.45
	0.7	100.06	24.68	117.19	467.05
1000	0.001	96.40	1.22	9.28	84.63
	0.1	96.38	1.87	17.52	239.08
	0.7	96.05	13.54	187.61	583.20

coordinate system whose Z axis is aligned with the normal to the orbit plane, $R_Z(-\Omega)R_X(-i)$ transforms the orbital coordinate system back to the inertial coordinate system.. \mathbf{r}'_1 and \mathbf{r}_0 are now forming a Lambert problem for a two-body orbit at t_0 . In this way, the secular effects of J_2 perturbation are more appropriately accounted for.

Now assume that there are two separate radar tracks of an object, and the IOD elements of the two tracks have been determined. After correcting positions of the second track for the J_2 secular effects using the IOD elements of the first track, we can now determine a set of orbital elements by solving the multiple-revolution Lambert problem with two positions from two tracks. The accuracy of the determined orbital elements will be much higher than that of the IOD elements.

However, in the real orbiting environment, in addition to the J_2 secular effects, the orbit is also affected by the short-periodic and long-periodic effects of J_2 perturbation. Considering that the maximum interval of LEO track association in this paper is 9 days, the magnitude of short-periodic effects is more significant than that of long-periodic effects according to the analytical perturbation theory of orbit.

Thus, we only consider the short-periodic effects in this paper. As mentioned earlier, the elements determined above using the Lambert problem are already accurate, they can be used to compute the short-periodic effects at the first and second tracks, and such corrected positions are again used to determine the orbital elements using the Lambert problem. In this way, the determined orbital elements are the mean elements at the epoch of the first track position.

2.2 Solution to Multiple-revolution Lambert Problem

Assume there are two two-body orbit position vectors \mathbf{r}_s and \mathbf{r}_e of an object which are separated by a transfer time $\Delta t = t_e - t_s$, one can obtain the displacement Δr and

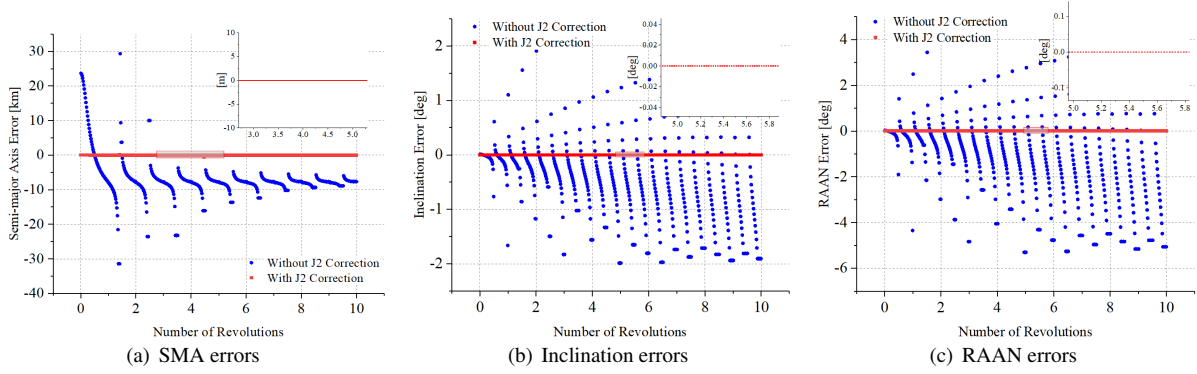


Fig. 5 Comparison experiment of J_2 correction.

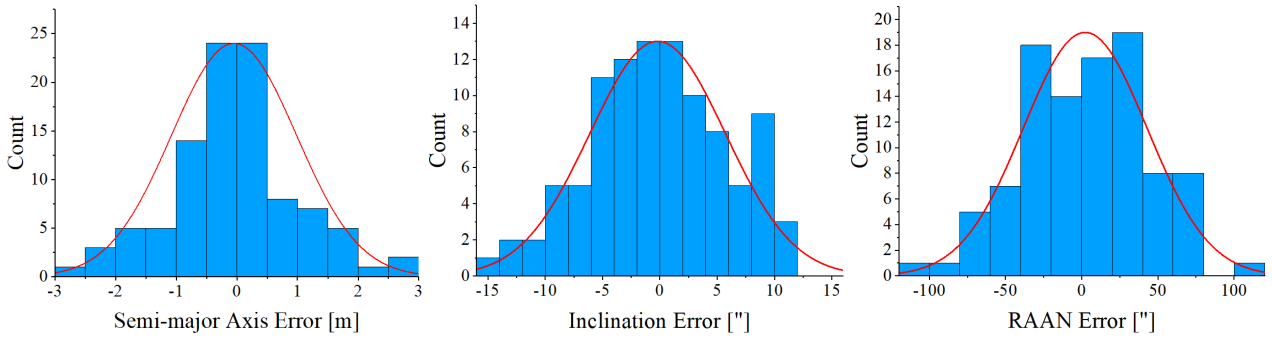


Fig. 6 Distribution of orbital element errors (when $H_{\text{perigee}} = 500$ km, $e = 0.001$).

transfer angle $\theta \in (0, \frac{\pi}{2})$ between r_s and r_e , expressed as

$$\begin{cases} \Delta r = r_e - r_s \\ \theta = \arccos \frac{r_e \times r_s}{|r_e| \cdot |r_s|} \end{cases} \quad (9)$$

With Δt as the input, the transfer two-body orbit parameters can be easily solved by Gooding method (Gooding 1990), if the two positions are in the same orbit revolution. There is either only a single solution or no solution by using the Gooding method. When the time interval between the two positions is longer than the orbit period of the object, the problem of multiple revolutions occurs. For the multiple-revolution Lambert problem, the transfer angle θ_{trans} is expressed as

$$\theta_{\text{trans}} = \begin{cases} \theta + m \cdot 2\pi \\ 2\pi - \theta + m \cdot 2\pi \end{cases}, \quad (10)$$

where θ is determined using Equation (9), and m is an integer representing the number of orbit revolutions over Δt , which is to be solved. In this case, there could be multiple solutions.

As shown in Figure 2, there are 4 orbital solutions to the multiple-revolution Lambert problem of two position vectors (r_1, r_2) given in Table 1, which are computed from the orbital elements $\{a = 7800.0$ km, $e = 0.001$, $i = 30^\circ$, $\Omega = 20^\circ$, $\omega = 40^\circ$, $M = 50^\circ\}$ at the epoch of r_1 . The solved 4 orbital elements are given in Table 2.

It can be seen that the two inclinations are complementary to 180° , and the two RAANs are apart by 180° . The orbital period (and thus the number of orbit revolutions over the time) and eccentricity of one solution are significantly different from those of another.

In summary, the number of orbit revolutions over the time interval Δt has to be determined to obtain the right solution. Therefore, there is a problem of orbit selection.

The main idea of determining the right orbit is to conduct O-C (Observed-Calculated) test, that is, the decision whether a selected orbit conforms to the true orbit is made based on the differences between observed tracks and tracks computed from the orbital elements.

As shown in Figure 3, given two radar observed tracks ($Track_1$ and $Track_2$, in black), we can obtain a number of orbits ($Orbit_1$ and $Orbit_2$, for example, in solid red and dash, respectively) by solving multiple-revolution Lambert problem of two positions from the two tracks. The positional differences between the observed tracks and a determined orbit are small if the determined orbit is close to the true orbit, and large otherwise. In this way, $Orbit_1$ is selected as the result orbit. The specific orbit selection procedure is given as follows. Assume we have obtained l sets of orbital elements by solving the multiple-revolution Lambert problem, $\{Ele_i, i = 1, 2, \dots, l\}$, where Ele_i is the i -th set of elements. Compute the differences between the observed positions and the positions computed

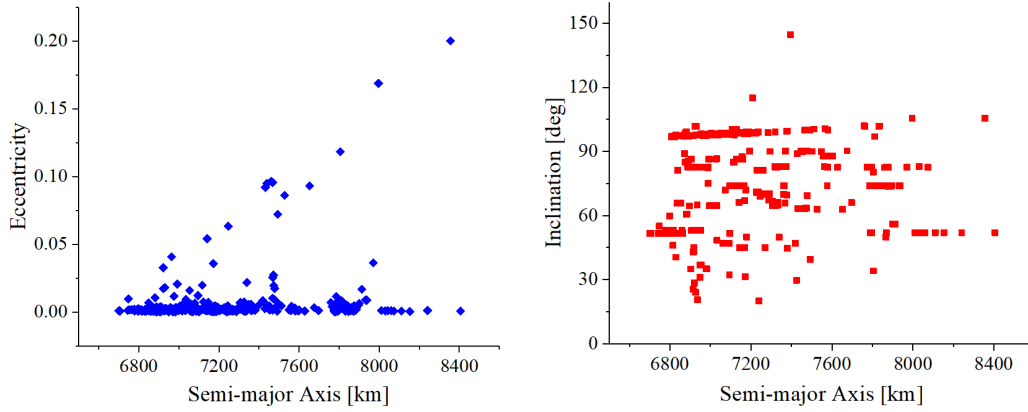


Fig. 7 Orbit Distribution of 889 LEO Objects.

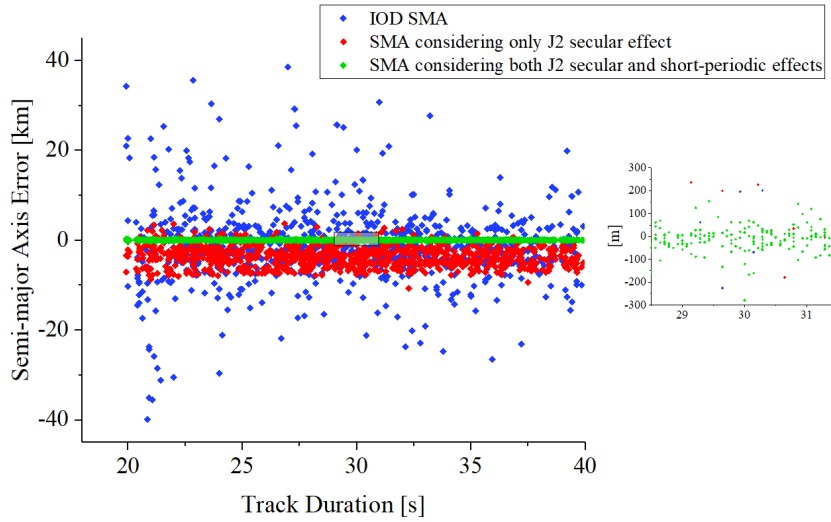


Fig. 8 Errors of the determined SMAs.

from Ele_i to result in 3 difference series in X , Y and Z , respectively, for each track. Each difference series is then fitted with a linear function. For each of the 3 difference series of a track, for example $\{\Delta X_i, i = 1, 2, \dots, m\}$, m is the number of data points of the track, and the following condition is tested to judge the closeness between the computed and observed positions, as

$$\begin{cases} \Delta X_{\max}, i \leq 1, 2, \dots, m \\ k < k_{\max} \end{cases}, \quad (11)$$

where k is the slope of the linear fitting function of $\{\Delta X_i, i = 1, 2, \dots, m\}$, ΔX_{\max} is the threshold for the difference, and k_{\max} is the threshold for the slope. If Equation (11) is satisfactory for all difference series of both tracks, the corresponding element set will be selected as the final result. The thresholds ΔX_{\max} and k_{\max} will be discussed in Section 3.

Table 5 Example of Orbit Accuracy Improvement

Orbit Height	First Track Duration	Δa_{IO}	$\Delta a_{\text{Secular}}$	Δa_{SP}
1355.6 km	21.0 s	51.9 km	2.62 km	44.9 m

2.3 Track Association

With the above approach that applying the Lambert problem to determine accurate orbital elements from two observed positions in two tracks, the association on two radar tracks can now be determined in the following manner. As shown in Figure 4, the two-track association algorithm is implemented as follows.

- 1) Determine the initial orbital elements of each track from its positions using the Lambert problem. Because the duration of a single track is usually only a few minutes or shorter, the track can be regarded as a two-body orbit.
- 2) Analytically propagate the IOD orbital elements of the first track to the epoch of the IOD orbital elements of the second track considering the J_2 secular effects. If

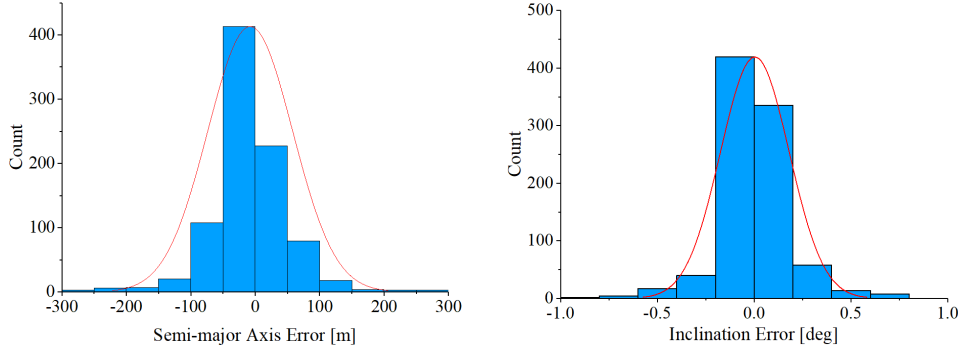


Fig. 9 Error distributions of determined mean SMAs (*left*) and inclinations (*right*) from only two first positions of two tracks.

the two tracks are from the same object, the propagated semi major axis should be close to the semi major axis of the second track, and the angle between the normal vector of the propagated orbit plane and the normal vector of the second track should be close to zero. Because of the errors in the observed positions, thresholds are assigned in the above comparisons. The thresholds should be set to allow two tracks from the same object being processed in the association, and also to reject two tracks apparently from two different objects. Considering the accuracy of the initial orbit elements determined from a single track varies greatly with the observation duration and accuracy, we set the deviation threshold 200.0km for difference between two SMAs and 5.0° for the angle between two IOD planes propagated to a common epoch. These settings are obtained from extensive experiments.

- 3) Pick the first position from the first track, denoted as P_1 , and the first position from the second track, denoted as P_2 . P_2 is corrected for the J_2 secular effects in the way described in Section 2.2. However, for the practical radar track association problem, only the IOD elements are available at the beginning. An iterative procedure is needed to determine accurate elements from the two positions.
 - 3.1) Use IOD elements of the first track to correct P_2 for the J_2 secular effects to result in P_2^1 . Then apply the method in Sections 2.2–2.3 to obtain a set of orbital elements at P_1 from (P_1, P_2^1) , denoted as Ele_1^0 .
 - 3.2) Repeat 3.1) using Ele_1^0 instead of the IOD elements to result in Ele_1^1 .
 - 3.3) Use Ele_1^1 to correct P_1 and P_2^1 for the J_2 short-periodic effects to result in P_1^2 and P_2^2 , respectively.
 - 3.4) Finally, apply the Lambert problem to (P_1^2, P_2^2) to obtain the mean elements at P_1 , and result in Ele_1^2 .
- 4) If the result orbit meets all the conditions of orbit selection in Section 2.3, the two tracks are declared

Table 6 Orbit Information for Single-object Association

Object	NORAD ID	a (km)	e	i ($^\circ$)
LEO1	45185	6923.66	0.00101	53.05
LEO2	39268	7137.17	0.05948	81.00
HEO1	14670	9773.29	0.30003	36.11

Table 7 Determined Orbital Elements from Two Radar Positions

Result Orbit	a (km)	e	i ($^\circ$)	Ω ($^\circ$)	ω ($^\circ$)	M ($^\circ$)
1	9235.8	0.31633	81.012	54.159	79.215	35.245
2	7991.6	0.15592	81.013	54.161	78.683	49.661
3	7132.1	0.05961	81.013	54.167	262.538	247.323
4	7363.3	0.45471	81.016	54.188	260.181	296.812
True Orbit	7131.9	0.05953	81.000	54.177	262.566	247.282

being from the same object. Otherwise, the two tracks are judged from two different objects.

3 EXPERIMENTAL RESULTS

The whole procedure to determine the association of two tracks involves a number of algorithms. In the following, these algorithms are validated and the two-track association performance is assessed through extensive simulation experiments.

3.1 Two-track Orbit Determination

3.1.1 Validation of orbit determination from two J_2 -perturbed positions

In order to validate Equation (8) of correcting position vector for the J_2 secular effects, we carried out a comparative analysis experiment. Assume that an object orbit has mean Keplerian elements at t_0 given in Table 3, and the orbit is affected only by the J_2 secular perturbation. Then the positions P_0 and P_1 , respectively at t_0 and $t_1 = t_0 + 0.02 \cdot l \cdot T + \delta t$, $l = 0, 1, \dots, 500$, $\delta t = 0.01 \cdot T$ (T is the orbit period), can be computed. Applying Equation (8) to correct P_1 for the J_2 secular effects, we obtain P_1' .

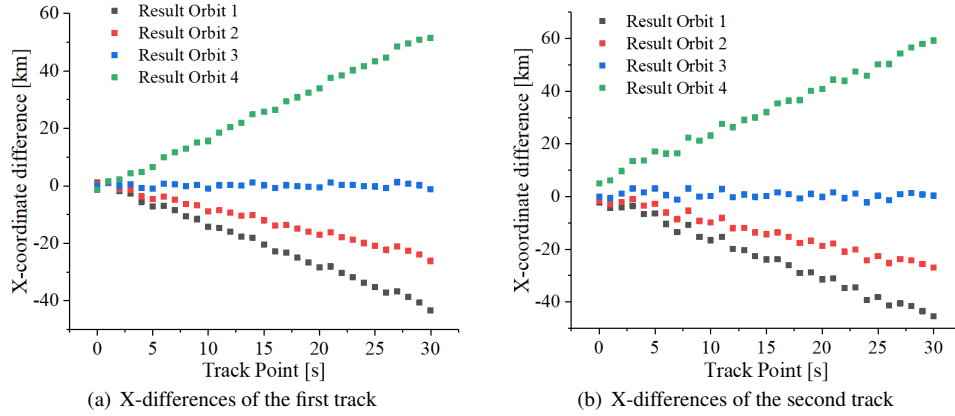


Fig. 10 Position differences between the calculated and observed tracks.

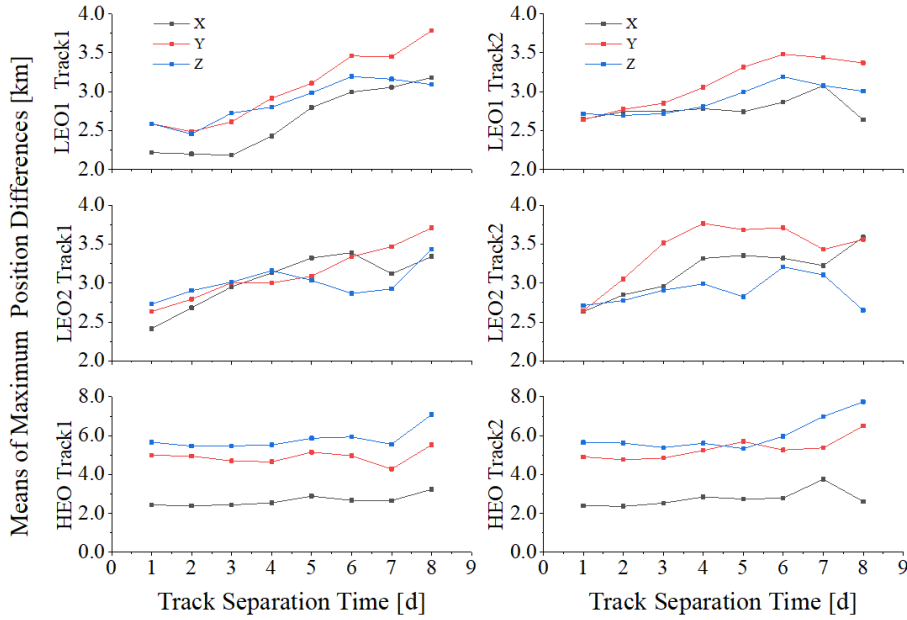


Fig. 11 Means of maximum position differences with respect to the best orbits. *Left*: the first track. *Right*: the second track.

Then, the Lambert problems for (P_0, P_1) and (P_0, P'_1) are solved using the Gooding method. The errors of the determined SMAs, inclinations and RAANs are shown in Figure 5.

As shown in Figure 5, if the correction is not made to the perturbed position P_1 , the errors in the determined SMAs, inclinations, and RAANs all have periodic changes. The magnitude of the SMA errors reaches a maximum when the time interval is $(p+0.5)T + \delta t$, $p = 1, 2, \dots, 9$. It is seen there is a mean bias about -8 km in the determined SMAs. For the errors of the determined inclinations and RAANs, their maximums are at the time interval $0.5 \cdot p \cdot T + \delta t$, $p = 1, 2, \dots, 9$. The inclination errors vary from -2 degrees to 2 degrees and the RAAN errors from -5 degrees to 4 degrees. These errors become larger with the increase of revolutions. On the other hand, if the J_2 secular

effects are corrected for P_1 , the mean orbital elements are determined exactly. The errors of the determined SMAs, inclinations, and the RAANs are all 0.

This experiment validates the method of correcting the perturbed position for the J_2 secular effects with Equation (8).

3.1.2 Orbit determination accuracy with two noisy positions

In practice, the radar measurements are noisy ranges and angles. As a consequence, the position computed with Equations (2)–(4) has error. It would be necessary to validate the method of orbit determination from two noisy positions. Experiments are designed to perform the validation.

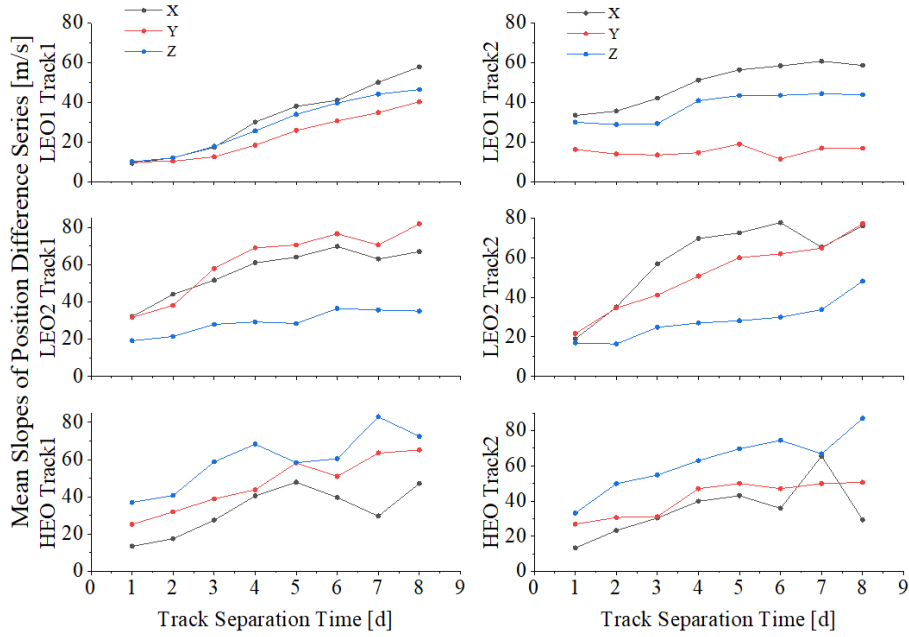


Fig. 12 Mean slopes of position difference series with respect to the best orbits. *Left*: the first track. *Right*: the second track.

Table 8 Two-track Association Experiment Results

Orbit Type	Perigee Altitude (km)	Tracks	NT	ND	NW	TP Rate (%)	Error Rate (%)
Total	243 – 4224	12142	249838	232745	4388	93.2	1.9
	< 500	2311	41674	38753	2761	93.0	6.7
LEO	500 – 700	3087	61336	57425	1198	93.6	2.0
	700 – 1000	3626	79069	73826	131	93.4	0.2
	> 1000	2716	64427	59700	280	92.7	0.5
HEO	-	402	3332	3041	18	91.3	0.6

Assume that the radar station is at a location of 120°E in longitude and 30°N in latitude, and the 1-sigma errors are 50 m and $100''$ for the measured ranges and azimuth/elevation angles, respectively. Orbits of varying perigee altitudes and eccentricities are assumed, and two positions separated by about 96–100 hours from each orbit are then “measured” by the radar. The information of simulated 9 orbits and the time intervals between two positions on each orbit is given in Table 4. It is noted that the orbits are affected by both the J_2 secular and short-periodic effects.

In the experiment, each orbit is independently measured 100 times at the two positions, and the two measured positions are then used to determine the orbital elements. The error RMSs of the determined 100 SMAs, inclinations and RAANs are listed in Table 4. Example error distributions of the determined SMAs, inclinations and RAANs are shown in Figure 6 for the orbit with perigee altitude 500 km and eccentricity 0.001. From Figure 6, it is seen that the errors of the determined SMAs and inclinations may be described by normal distributions

of zero mean. By Kolmogorov-Smirnov test, the P-values of SMAs error and inclination error series are 0.608 and 0.920 respectively, which are in line with normal distribution.

Examination of Table 4 reveals that, when the orbit becomes more eccentric, the errors of the determined elements increase too. When the perigee height of the object orbit is 500 km and the eccentricity is 0.001, the error RMSs of the SMA and the inclination are 1.02 m and $5.87''$, respectively. For the orbit of the same perigee altitude but a larger eccentricity of 0.1, they grow to 1.53 m and $9.68''$, respectively. They are still only 10.19 m and $203''$, respectively, when the eccentricity becomes 0.7. However, the error RMS of the RAAN is significantly larger. The results of other orbits all have the similar characteristics.

As a whole, the accuracy of the orbit determination from two noisy positions is acceptable for our purpose of track association, as evidenced in the following. The developed method is suitable for determining orbital

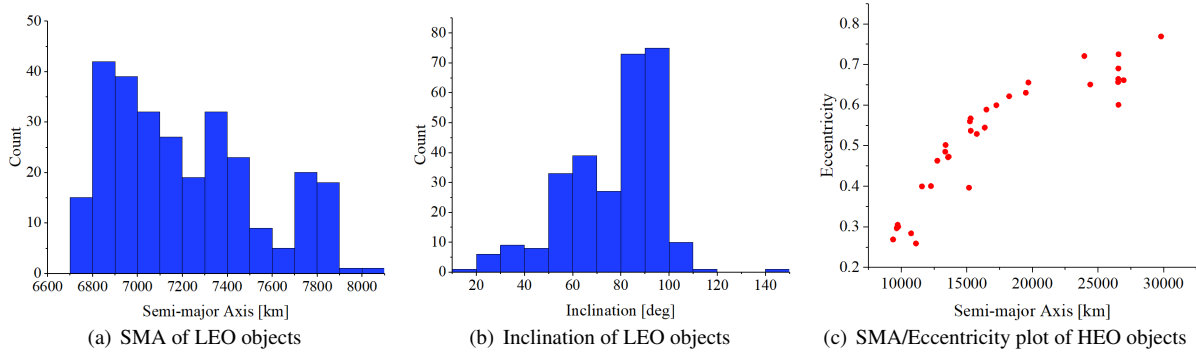


Fig. 13 Orbital element distribution of experiment objects.

Table 9 Slope Thresholds and Track Association Results

Slope threshold(m/s)	NT	ND	NW	TP rate(%)	Error rate(%)
90.0	249838	231029	3914	92.47	1.67
100.0	249838	232745	4388	93.16	1.85
110.0	249838	234152	5077	93.72	2.12

elements from radar observations of LEO objects on orbits of varying heights and eccentricities.

3.1.3 Orbit determination with two radar tracks

In the above experiments, the mean orbital elements at t_0 are known exactly. However, to associate two radar UCTs, the accurate mean elements are not available at the beginning. We can only obtain a set of IOD elements for a UCT. Whether the IOD elements of the first UCT are accurate enough to remove the J_2 effects in the observed positions needs further verification. For this, radar tracking simulations are performed.

The radar data accuracy is again set to 50 m for ranges, and $100''$ for angles. The radar station longitude and latitude are 115°E and 30°N , respectively. The “true” orbits of 889 LEO objects, which are all NORAD objects, are determined using the method described in Chen (2017), which considers the gravity field (50/50 order/degree JGM-3), lunisolar perturbations, solar radiation pressure and atmospheric drag (DTM78 atmospheric mass density model). The orbit distribution of these LEO objects is shown in Figure 7.

Given the “true” orbits of the LEO objects, radar tracks can be measured. In this experiment, the track durations are set to not longer than 40 s. For each of the 889 objects, a track on the first day and another track on the fourth day are chosen to determine the mean elements of the first track of the object. The first position from the first track and the first position from the second track are picked, which form the Lambert problem for the two positions. Then the procedure described in Step 3) in Section 2.3 is applied to obtain a set of mean orbital elements at the epoch of the first position in the first track.

Table 5 presents an example of determined SMA errors by applying the proposed method. The IOD SMA of the first track of 21 s in duration has an error of 51.9 km. When the IOD elements of the first track is used to correct the J_2 secular effects in the first position of the second track, the error of the determined SMA from the Lambert problem is reduced to 2.62 km. After further considering the short-periodic effects, the error of the determined mean SMA is only 44.9 m. The example also demonstrates that the larger IOD errors have little effect on the two-track orbit determination accuracy.

For the simulated 889 objects, the proposed method is applied and orbital elements are determined for each of them. The scatter plot of errors of the determined SMAs is shown in Figure 8, and Figure 9 presents the error distributions of the determined mean SMAs and inclinations.

It can be seen from Figure 8 that the IOD SMA errors from single tracks are basically within 40 km (there are a few of them outside the 40 km boundary), and the long track duration generally results in accurate IOD estimate. When the two first positions from two tracks are solved for the orbital elements in which only the J_2 secular effects are considered, the SMA errors are reduced to less than 10 km. And they are further reduced to less than 200 m after considering the short-periodic effects.

It is noted from Figure 8 and the left of Figure 9 that the errors of the determined mean SMAs are randomly distributed with the mean equal to -7.7 m, and the error RMS is 66.74 m. The SMAs determined considering only the J_2 secular effects have a mean bias of -3.27 km. The right panel of Figure 9 shows that the errors of the determined mean inclinations are closely centered around zero with a mean of $12''$ and RMS of 0.18° . By Kolmogorov-Smirnov test, the SMA and inclination errors in Figure 9 do not conform to normal distribution.

Therefore, the proposed method is shown to be able to determine accurate orbital elements from two radar positions separated by less than 4 days.

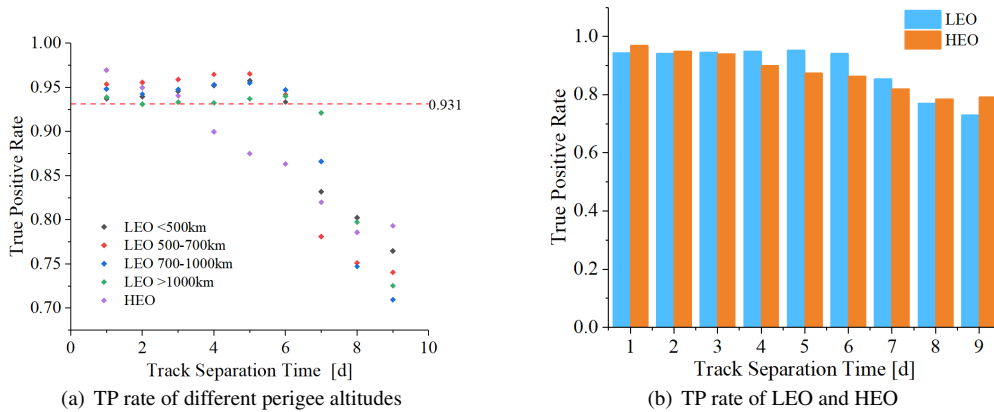


Fig. 14 True positive rate with track separation time.

3.2 Track Association

We have demonstrated in the above that, given two tracks of an object separated by a few days, the proposed method can accurately determine the orbital elements of the object. We now explore its excellent ability to perform two-track association.

Solving the Lambert problem from two positions would result in a number of orbital element sets. Each set is tested using the differences between the observed and computed positions for both tracks. It is understandable that, if an estimated element set is close to that of the true orbit, the differences, which form three series in the X , Y , and Z coordinates for each track, will all be small. If the two tracks are from two different objects, either the Lambert problem has no solution or the solved solutions would highly likely make the differences large. In other words, if the differences in all 6 series for the two tracks are small, it is highly likely that the two tracks are from the same object. The magnitude of the differences is clearly dependent on the closeness between the determined and observed tracks. In a summary, the prerequisite to have small differences is to have accurate orbital elements.

In the following, example difference series resulted from the multiple-revolution Lambert problem solutions to two positions are presented first to see the variations of the differences with solved orbital elements. The thresholds for judging the position differences small or large are then determined. Finally, two-track association experiment is made for thousands of LEO and HEO tracks and the performance is assessed.

3.2.1 Analysis on position differences

In this experiment, two LEO objects and a HEO object, whose orbit information is given in Table 6, are selected for the position difference analysis. Tracks having a duration from 20 s to 30 s are generated over a 9-day time span for the 3 objects. The 1-sigma range and angle errors are again

50 m and $100''$, respectively. Given two independent tracks of an object, the Lambert problem of the two first positions from the two tracks is solved, and the differences between the observed and computed positions are determined.

Figure 10 shows the difference series in the X coordinate for two tracks of LEO2 object, here the first track and the second track have a separation time of 9.34 hours. Given these two tracks, solving the Lambert problem of the two first positions results in 4 sets of orbital elements, as shown in Table 7. Figure 10 shows that the differences computed from Orbit 3 are close to zero for both tracks. On the other hand, all other difference series appear as lines which have obvious slopes, and it is clear that the differences grow quickly with time if the determined orbit is not close to the true orbit. From the difference series, it is easy to determine that, among the four solved orbits, Orbit 3 is the best estimate to the true orbit.

Because a difference series over the track duration appears as a line, it can be fitted with a linear function. From Figure 10, the estimated slope appears a quality metric to determine the closeness between a solved orbit and the true orbit. In addition, the maximum value in the difference series seems another metric to this closeness determination. For each of the 3 objects in Table 7, many two-track combinations can be formed, and each combination is solved for the orbital elements. All the solutions are grouped in terms of the track separation time, and for each group, the mean values of the difference maximums and of estimated slopes corresponding to the best orbits, are shown in Figures 11 and 12, respectively.

Observing Figure 11, one can see that the means of maximum differences are all less than 4 km for all two-track combinations of the two LEO Objects. They are less than 8 km for the HEO object. The means of maximums of the first tracks are generally at the same level as those of the second tracks. The magnitude of the means increases slowly with the track separation time. On the other hand,

the slopes increase at a faster pace, but they are all smaller than 90 m/s as shown in Figure 12.

From these maximums of position differences and estimated slopes of difference series, the decision thresholds for two-track association can be set to 20 km for the differences in all coordinates and 100 m/s for the slopes of the difference series. The 20 km threshold for the position differences and the 100 m/s for the slopes can separate with a high confidence the best orbit from other multiple-revolution Lambert problem solutions, as shown in Figure 10.

3.2.2 Multi-object association experiment

Given the thresholds determined above, extensive two-track association experiment can now be performed. A two-track association will result in either a true or false decision. As a matter of fact, there are 4 decision scenarios: true positive (TP) if two tracks are from the same object and the association says so; false negative (FN) if two tracks are from two objects and the association says so; true negative (TN) if two tracks are from the same object but the association says they are not from the same object; false positive (FP) if two tracks are from two objects but the association says they are from the same object. For the practical applications, the most important issue is to correctly associate any two tracks from the same object, that is, the TP rate is the most critical measure to assess the performance of a two-track association method. In order to assess the performance of the two-track association method proposed in this paper, we carried out a simulation experiment involving 283 LEO objects and 34 HEO objects, with the SMA and inclination distributions of LEO objects, as well as the SMA/eccentricity distribution of HEO objects shown in Figure 13.

The radar station is still at 115°E in longitude and 30°N in latitude, and the ranging and angles accuracy are 50 m and 100'', respectively. Over a 9-day time span, a total of 12142 tracks are observed for the 317 objects, with the track durations ranging from 20 s to 40 s. Any of the 317 objects has at least 2 tracks over the time span. Each two-track combination of the total 73,708,011 is processed to determine the association. It only took 40 minutes to complete the computation. The TP rates of the two-track association operation are given in Table 8, where NT stands for the number of total two-track combinations from the same object, ND the number of correctly determined two-track combinations from the same object, and NW the number of FP decisions. The TP rate is computed as ND/NT , and the error rate is computed as $NW/(ND+NW)$.

The overall TP rate over the 9-day time span, seen from the first row of Table 8, is 93.2%, which is an excellent result considering that the objects are at orbits of different altitudes and eccentricities, and the track

separation can be as long as 9 days. Looking further into various scenarios of orbits and track separation times would reveal more details of the association performance. We divide the LEO objects into 4 groups in terms of the perigee altitude. The TP rates and error rates for the 5 object groups including the HEO objects are given in Table 8. It is seen that the TP rates for associating two LEO tracks in all LEO groups are better than 92.7%. The TP rate for associating two HEO tracks is 91.3%. In terms of error rates, the LEO objects lower than 500 km hold the largest error rate of 6.7%, while the error rate of objects with height between 700–1000 km is as low as 0.2%. The error rate of HEO is 0.6%.

The TP rate of two-track association is shown in Figure 14 as a function of track separation time, where the separation time is regarded being 1 day if it is less than 1 day, 2 days if it is between 1 and 2 days, and so on. It is clear that, the TP rates of LEO and HEO demonstrate difference change behaviors with the increasing of separation time. For the LEO objects, the TP rates remain relatively steady and consistently higher than 93.1% when the separation time is less than 6 days, then it decreases sharply thereafter to between 70.9% and 76.5% when the separation is 8–9 days. While the TP rate of associating HEO tracks decreases almost linearly with the separation time from 96.9% at 1 day to about 78.6% at 8–9 days. Figure 14(b) demonstrates that two LEO tracks from the same object apart by less than 6 days can be correctly associated with a probability of 94.2%, and two HEO tracks separated by less than 3 days with a probability of 94.0%.

It is worth noting that the TP rate varies with the thresholds on the coordinate difference and difference slope. Experiments have shown that, when the slope threshold is increased or reduced by 10% from used 100 m/s, the TP rate and error rate are changed by less than 1%, as shown in Table 9.

It can be seen that when the slope threshold is set to 90 m/s, the error rate decreases by a small percentage, but the TP rate decreases too. When the threshold is set to 110 m/s, the TP rate increases but the error rate increases too. From these results, we think that the current thresholds are appropriate.

4 CONCLUSION

In this paper, a set of algorithms to associate two radar tracks based on the Lambert problem is developed, and they are assessed by extensive simulation experiments.

The standard Lambert problem is only applicable to two positions on a two-body orbit. However, the observed orbit is affected by various perturbations. Therefore, it is a prerequisite that the observed positions have to be corrected for the perturbation effects in order to apply the Lambert problem. Considering that the J_2 term is the

dominant perturbation for LEO and HEO objects and that only the initial orbital elements can be determined from single tracks of a new object, a procedure to account for the J_2 secular and short-periodic effects on the observed positions is proposed. Following this procedure, a two-track association method, which corrects the secular and short-periodic effects of J_2 perturbation and exclusively applies the Gooding method to solve the Lambert problem, is developed. The best orbit is determined from multiple-revolution orbit solutions using observed positions on both tracks.

Extensive experiments are performed and the proposed algorithms are thoroughly validated. The orbit determination by solving the Lambert problem of two positions from two tracks of the same object demonstrates that the mean semi major axis can be estimated with an accuracy about 66.7 m, and the inclination with 0.18° when the range and angles errors are 50 m and $100''$, respectively.

With accurately determined orbital elements, the two-track association becomes a relatively easy work. Experiments involving 283 LEO objects and 34 HEO objects show that, the overall true positive rate is 93.2%. The TP rate of associating two LEO tracks separated by less than 6 days is 94.2%, and it is 73.1% even when the track separation time is 8–9 days. The TP rate for HEO track association is lower than that for LEO tracks, but it is still at 94.0% when the separation is less than 3 days, and 78.6% when the separation is 8–9 days. These TP rates are comparatively better than those reported by Reihls et al. (2020) which uses Mahalanobis distances to perform association of two radar tracks.

In the future work, the proposed algorithms will be tested to associate real radar tracks and the results will be reported when available.

Acknowledgements The authors would acknowledge the research support from the National Natural Science Foundation of China (Grant No. 41874035), the Natural Science Foundation of Hubei province, China (Grant No. 2020CFB396), and the Fundamental Research Funds for the Central Universities, China (Grant No. 2042021k-f0001). The authors are grateful to anonymous reviewers whose constructive and valuable comments greatly helped us to improve the paper.

References

- Agapov, V. M. 2001, Space Objects Data Catalogue, in Space Debris, ESA Special Publication, 2, ed. H. Sawaya-Lacoste, 759
- Andrew, A. L. 1975, *Technometrics*, 17, 277
- Battin, R. H. 1977, *AIAA J.*, 15, 707
- Chen, J. Y., Li, B., & Sang, J. Z. 2017, Orbit Improvement and Re-cataloging of Catalogued Objects Based on TLE Data, in 2nd China Aerospace Safety Conference Series (in Chinese)
- Escobal, P. R. 1969, *Methods of astrodynamics*, (London: John Wiley)
- Feng, H. Y., Yue, X. K., & Wang, X. C. 2021, *Acta Aeronautica et Astronautica Sinica*, 42, 324699 (in Chinese)
- Gooding, R. H. 1990, *Celestial Mech. Dyn. Astron.*, 48, 145
- Gronchi, G. F., Baù, G., & Marò, S. 2015a, *Celestial Mechanics and Dynamical Astronomy*, 123, 105
- Gronchi, G. F., Dimare, L., Bracali, C. D., & Ma, H. 2015b, *MNRAS*, 451, 1883
- Ha, S. N. 2001, *Computers & Mathematics with Applications*, 42, 1411
- Hill, K., Sabol, C., & Alfriend, K. T. 2014, *Journal of the Astronautical Sciences*, 59, 281
- Huang, J., Hu, W. D., Xin, Q., & Du, X. Y. 2012, *RAA (Research in Astronomy and Astrophysics)*, 12, 1402
- Izzo, D. 2015, *Celestial Mechanics and Dynamical Astronomy*, 121, 1
- Jiang, H., Liu, J., Cheng, H. W., & Zhang, Y. 2017, *RAA (Research in Astronomy and Astrophysics)*, 17, 30
- Lee, E., Park, S.-Y., Hwang, H., Choi, J. et al., 2020, *Acta Aeronautica*, 176, 247
- Lei, X. X. 2021, *Acta Geodaetica et Cartographica Sinica*, 50, 283 (in Chinese)
- Lei, X. X., Wang, K. P., Zhang, P., et al. 2018, *Advances in Space Research*, 62, 542
- Liu, L. 2006, *An introduction of astrodynamics* (Nanjing: Nanjing Univ. Press)
- Liu, L., Chen, J., Lei, X., et al. 2020, in *Sixth Symposium on Novel Photoelectronic Detection Technology and Application*, Proc. SPIE 11455, 1145502
- Ma, H., Baù, G., Bracali, C. D., & Gronchi, G. F. 2018, *Celestial Mechanics and Dynamical Astronomy*, 130, 70
- Maruskin, J. M., Scheeres, D. J., & Alfriend, K. T. 2009, *Journal of Guidance Control Dynamics*, 32, 194
- Memon, S. A., Song, T. L., Memon, K. H., & et al. 2020, *Expert Systems with Application*, 141, 112969
- Reihls, B., Vananti, A., & Schildknecht, T. 2020, *Advances in Space Research*, 66, 426
- Vallado, D. A., & McClain, W. D. 1997, *Fundamentals of Astrodynamics and Applications* (Berkshire: McGraw-Hill Publishing Company)
- Vananti, A., Schildknecht, T., Siminski, J., Jilete, B., & Flohrer, T. 2017, Proc. 7th European Conference on Space Debris, <https://conference.sdo.esoc.esa.int/proceedings/sdc7/paper/925/SDC7-paper925.pdf>
- Xu, X.-L., & Xiong, Y.-Q. 2014, *RAA (Research in Astronomy and Astrophysics)*, 014, 601